Published as: *Nature*. 2012 October 11; 490(7419): 226–231.

A Neural Circuit for Spatial Summation in Visual Cortex

Hillel Adesnik[1,2], **William Bruns**[1], **Hiroki Taniguchi**[3], **Z. Josh Huang**[3], and **Massimo Scanziani**[1]

[1]Howard Hughes Medical Institute, Center for Neural Circuits and Behavior, Neurobiology Section and Department of Neuroscience, University of California San Diego, La Jolla, California 92093-0634, USA

[3]Cold Spring Harbor Laboratory, 1 Bungtown Road, Cold Spring Harbor, NY 11724, USA

Abstract

The response of cortical neurons to a sensory stimulus is modulated by the context. In the visual cortex, for example, stimulation of a pyramidal cell's receptive field surround can attenuate the cell's response to a stimulus in its receptive field's center, a phenomenon called surround suppression. Whether cortical circuits contribute to surround suppression or whether the phenomenon is entirely relayed from earlier stages of visual processing is controversial. Here we discover that, in contrast to pyramidal cells, the response of somatostatin expressing inhibitory neurons (SOMs) in the superficial layers of the mouse visual cortex increases with stimulation of the receptive field surround. This difference results from SOMs' preferential excitation by horizontal cortical axons. By perturbing SOMs' activity, we demonstrate that these neurons contribute to pyramidal cells' surround suppression. These results establish a cortical circuit for surround suppression and attribute a particular function to a genetically defined type of inhibitory neuron.

Visual stimuli located outside of the classical receptive field of a neuron in visual cortex while unable to elicit spiking may modulate the neuron's response to stimuli located in its receptive field [1–3]. Surround suppression, a basic operation in visual processing, is a classical example of this type of modulation [4–9] and can be easily observed when monitoring the firing of a neuron to a stimulus of increasing size centered on its receptive field (i.e. the size tuning of the neuron): The neuron's initial increase in firing is followed by a decrease as the stimulus becomes progressively larger. This form of suppression has been suggested to contribute to a number of perceptual effects like pop-out, curvature detection and orientation discrimination [8, 10–12]. Importantly surround suppression is not only observed in the cortex but is already present at earlier stages along the visual hierarchy namely in the retina [13, 14] and the thalamus [15–17]. Thus while it is likely that at least part of suppressive surround observed in the cortex is relayed from earlier stages of visual processing [18], some experimental observations and theoretical models suggest that the cortex is itself capable of contributing to surround suppression [19–21]. Below we reveal the identity and describe the mechanism of a cortical circuit that directly contributes to surround suppression in the superficial layers of primary visual cortex.

Correspondence: Massimo Scanziani, Neurobiology Section, mail code 0634, University of California, San Diego, 9500 Gilman Drive, La Jolla, CA 92093-0634, massimo@ucsd.edu.
[2]Present address: Department of Molecular and Cellular Biology and the Helen Wills Neuroscience Institute, University of California, Berkeley

Author Contributions: H.A. and M.S. designed the study. H.A. conducted all experiments. W.B. conducted all *in vivo* data analysis and spike sorting. H.T. and Z.J.H. generated the SOM-IRES-CRE mice. M.S. and H.A. wrote the paper.

Different size tuning of distinct neurons

We determined the tuning to the size of a visual stimulus for neurons in the superficial layers of the primary visual cortex (V1; depth ~100–350 μm, corresponding approximately to layer 2/3) of mice. Experiments were performed in awake, running animals, as size tuning was affected by anesthesia (Suppl. Fig. 1). Mice were head fixed but otherwise unrestrained and free to run on a passive circular treadmill. For behavioral consistency all data presented here were recorded during running events (see methods).Visual stimuli were composed of circular patches of drifting gratings at maximal contrast presented at 6–7 different sizes (from 8 – 96 degrees in diameter, Fig. 1a). The size-tuning curve of isolated units [22] (n=53; Suppl. Fig 2), i.e. the neuronal firing rate as a function of stimulus size, peaked at 22±2 degrees (preferred size) and progressively decreased with larger stimuli (Fig. 1a,d), revealing marked surround suppression [23] (average firing rates (FR): at baseline (FR_{BL}): 0.47±0.11 Hz; to smallest stimulus (FR_{SS}): 3.0 ±1.0 Hz, to preferred stimulus (FR_{PS}): 3.1± 0.3 Hz; to largest stimulus (FR_{LS}): 1.0±0.2 Hz; stimulus modulation index (SMI, computed as (FR_{PS} - FR_{BL}) / FR_{PS}): 0.87±0.03). The suppression index (SI), i.e. the difference between the peak response and the response to the largest stimulus, divided by the baseline subtracted peak response ((FR_{PS} - FR_{LS})/(FR_{PS} - FR_{BL}); Fig. 1a) averaged 0.9±0.1 (n=53; SI statistically significant in 33/53 units; permutation test; Fig. 1d), indicating substantial suppression to large stimuli. Infrequent eye- movement occurring during running had little effect on the size tuning curve (Suppl. Fig. 3).

If cortical circuits contribute to surround suppression they may involve the suppressive action of cortical inhibitory neurons. An inhibitory neuron lacking surround suppression and whose response increases with stimulus size would be a good candidate. In cats visual cortex, for example, fast spiking inhibitory neurons responding with higher firing rates to large as compared to small visual stimuli [21]. We performed targeted loose patch recordings from inhibitory neurons in layer 2/3 of V1 in awake, running mice, using two photon laser scanning microscopy [24] (Fig.1b,c). Parvalbumin expressing neurons (PVs) [25], a large class of cortical inhibitory neurons, were visualized in layer 2/3 by crossing a PV-Cre mouse line with a tdTomato reporter line. The size tuning curve of PVs peaked at 57±8 degrees (n=11) and showed marked surround suppression with larger stimuli (SI: 0.46±0.12 ; n=11; SI statistically significant in 6/11 cells; permutation test; Fig 1b,e; FR_{BL}: 9±2 Hz; FR_{SS}: 27±7 Hz; FR_{PS}: 45±11 Hz; FR_{LS}: 26±8 Hz; SMI,: 0.74 ± 0.07; recorded PVs showed their characteristic “thin” spikes shapes (Suppl. Fig. 2), confirming the accuracy of our targeting strategy [22, 26]). In striking contrast to PVs, somatostatin expressing neurons (SOMs), another large class of cortical inhibitory neurons [25] (visualized by crossing a SOM-Cre line with a tdTomato-reporter line [27]), completely lacked surround suppression (SI: 0.09±0.06 ; n = 8; SI stat. sign. in 0/8 cells ; permutation test; significantly different from PVs; $p<0.03$, rank sum test; Fig. 1f). The size tuning curve of these neurons showed a monotonic increase or saturation in firing rate with stimulus size (Fig 1c,f). While the smallest stimuli were relatively inefficient in driving SOMs (FR_{BL}: 7±2 Hz; FR_{SS}: 5±2 Hz), they robustly responded to large stimuli (FR_{PS}: 26±2 Hz; preferred size: 86±3 degrees; different from PV, $p<0.015$, rank sum test; SMI: 0.75±0.05). These data demonstrate that in V1 size tuning can be very different between genetically distinct types of neurons. Furthermore, these data suggest that SOMs are potential candidates in the generation of cortical surround suppression.

Excitation of SOMs by horizontal axons

The above observations open two fundamental questions: First, what are the cortical circuits that enable SOMs, in contrast to other cortical neurons, not to be suppressed but rather

facilitated by large stimuli? Second, do SOMs contribute to size tuning in V1? Both questions are addressed below.

The two predominant excitatory inputs to layer 2/3 are vertically ascending axons from layer 4 and horizontal projecting axons from layer 2/3. Are SOMs equally excited by these two inputs? We recorded from layer 2/3 pyramidal cells (PCs), SOMs and PVs in coronal slices of V1 and selectively photo-activated (light ramp of 2s duration; 480 nm light) layer 4 excitatory cells that conditionally expressed Channelrhodopsin-2 [28] (ChR2; Suppl. Fig 4). Layer 4 photo-stimulation generated excitatory charges in SOMs that were only 17 ± 5% (n=8) of those in simultaneously recorded PCs (Fig. 2a); in contrast, excitatory charges generated in PVs were 250 ± 39% (n=8) of those generated in simultaneously recorded PCs (Fig. 2b). These results were corroborated through ChR2-assisted circuit mapping [29] (Suppl. Fig. 5). Thus, ascending layer 4 axon provide little excitation to SOMs. In striking contrast, photo-stimulation of layer 2/3 PCs (2 s light ramp duration) that selectively expressed ChR2 (see methods [30]) produced substantial excitation of layer 2/3 SOMs (Fig 2d): the excitation that SOMs received was in fact significantly larger than that received by simultaneously recorded PCs (241 ± 85%; n=7; $p<0.05$; Fig. 2e; we selectively recorded from those PCs not expressing ChR2 in order to avoid contamination with photocurrents; [30]). Furthermore, while photo-stimulation of horizontal layer 2/3 projections was accompanied by strong disynaptic inhibition in PCs, only very little inhibition was recorded in SOMs (Fig. 2e; the ratio of excitation to the sum of excitation and inhibition (E/(E+I)) was 0.11 ± 0.01 (n=10) in PCs versus 0.59 ± 0.06 (n= 11) in SOMs; $p<0.05$, Fig. 2f). Thus, these results show that while layer 2/3 pyramidal and PVs receive substantial excitatory drive from ascending layer 4 axons, the main excitation to layer 2/3 SOMs are horizontal axons of layer 2/3.

Size-dependent excitation of SOMs

To ascertain that these horizontal axons are indeed responsible for the size-dependent recruitment of SOMs, we took advantage of the retinotopic organization of V1[31]; we reasoned that because progressively larger visual stimuli presented *in vivo* will result in a progressively larger visually activated area in V1 we could approximate this expansion of activity by directly photo-stimulating progressively larger areas of V1. We performed loose patch recordings from SOMs in coronal slices of V1 expressing ChR2 in layer 2/3 PCs (Fig 3a). The firing rate of SOMs increased as a function of the size of the light spot (range of sizes 180–900 μm), similar to their increase in firing rate *in vivo* with increasing visual stimulus size (Fig. 3a,b). Consistent with the increase in firing rate, the synaptic excitation received by SOMs increased with increasing light spot size (Fig. 3a,b). If SOM dendrites were to span areas similar to the largest light-spot diameter, the progressive increase in firing rate with spot size could simply result from the direct photo-stimulation of synapses on the dendritic arborization of the recorded SOM. This was however not the case because even the smallest light spot used (180 μm diameter), generating only ~25% of the maximal firing rate, covered already more than 95% of the entire SOM dendritic arborization (Fig. 3b, see methods). Thus, the increase in SOM firing rate with spot size results from the recruitment of progressively more distant L2/3 PCs (Fig. 3b, see methods). Furthermore, cutting horizontal axons with two vertical cuts through layer 2/3 on each side of the recorded SOMs (320 ±25 μm between cuts, centered on the cell; n=10; note that the distance between the cuts is larger than the horizontal dendritic extent of SOMs) prevented the increase in firing rate with stimuli larger than the distance between the two cuts (Suppl. Fig. 6). Thus, by using horizontal layer 2/3 projections as their main excitatory drive, SOMs are recruited as a function of the activated V1 area, that is they sum activity in visual space.

Is the size-dependent recruitment of SOMs a mechanism that could contribute to the suppression of PC firing to large stimuli? We recorded from PCs in coronal slices of V1

conditionally expressing ChR2 in layer 2/3. The firing rate of PCs was set to ~10 Hz by direct current injection (Fig. 3c). A small light spot centered around the recorded PC reduced the firing rate and this suppression became progressively more pronounced as a larger area of layer 2/3 was activated by increasing the size of the light spot (Fig. 3c). Consistent with the progressive suppression in firing rate, the inhibition received by PCs increased with increasing light spot size (Fig. 3c,d). Finally, to establish that the inhibition generated in PCs upon photo activation of layer 2/3 [30] was indeed due to the recruitment of SOMs [32] and not any other interneuron type we optogenetically silenced SOMs (see methods) while monitoring the inhibition in PCs during photoactivation of layer 2/3 (Fig. 3e). Photo-stimulation of layer 2/3 to activate PCs generated strong firing in SOMs and large inhibitory currents in simultaneously recorded PCs, consistent with the results reported above (Fig. 3e). Strikingly, concomitant optogenetic silencing of SOMs (100% reduction of firing; n= 6) strongly reduced the inhibitory currents in PCs (80 ± 4% reduction; n=8 $p<0.05$, Fig. 3e,f).

Thus, the stimulus-size dependent recruitment of SOMs generates strong inhibition in layer 2/3 PCs and efficiently suppresses their firing rate (Fig. 3g).

SOMs contribute to surround suppression

These data provide a plausible mechanism by which SOMs could contribute to surround suppression of layer 2/3 PCs in vivo. Furthermore, consistent with a possible contribution of SOMs to surround suppression, under anesthesia, a situation in which surround suppression is compromised (see above and Suppl. Fig. 1) the firing rate of SOMs was reduced ten fold (from 26 ± 2 Hz, n=8 to 2.7± 0.4 Hz, n= 10), much more than that of single units or PVs (Suppl. Fig. 1). To directly test for the involvement of SOMs in surround suppression we conditionally expressed the light-sensitive hyperpolarizing opsin archaerhodopsin (Arch)[33] in V1 using viral injection of a flexed Arch vector[34] into SOM-Cre mice (71 ± 2% of cells infected, n = 4 animals, Fig. 4b and see methods). Illumination of the cortical surface efficiently reduced the visually evoked activity of Arch-expressing layer 2/3 SOMs (80 ± 1% suppression, n = 4, $p<0.05$; Supp. Fig. 7),. To determine the impact of SOMs on size tuning in layer 2/3 we performed extracellular recordings as described above and alternated control trials (visual stimulus only) with trials in which SOMs were photo-hyperpolarized (Fig. 4). Photo-hyperpolarization of SOMs significantly reduced surround suppression of layer 2/3 neurons by 30 ± 10% (n=28; $p < 0.00022$, paired signed rank test; Fig.4c-e; photo-hyperpolarization of SOMs had no significant effect on baseline firing rates −9±17%; n=13; $p>0.18$). Nearly all units (25/28) showed a decrease in SI (Fig. 4e) and in 10/25 units the decrease was individually significant ($p< 0.05$ permutation test). The reduction of SI resulted from the fact that SOM photo-hyperpolarization facilitated the response to large visual stimuli more than to small visual stimuli: The response ratio (the ratio of the firing rate in the illumination condition divided by firing rate in the control condition) increased with the size of the stimulus (Fig. 4f). Indeed, while the response to stimuli smaller or equal to the preferred size was not facilitated (−7± 7%, $p > 0.45$, paired signed rank test; n=28; $FR_{PS, CTRL}$ = 4.9 ± 1.5 Hz, $FR_{PS, LED}$ = 4.6 ±1.9 Hz, $p >0.63$, paired signed rank test) the response to the stimuli larger than the preferred size was facilitated by 74±19 % ($p<0.0011$, paired signed rank test; n=28; Fig. 4f). This lack of facilitation of responses to smaller visual stimuli was not due to saturation (i.e. a ceiling effect). In fact, firing rates to stimuli smaller or equal to the preferred one were consistently facilitated less than similar firing rates elicited by stimuli larger than the preferred one (Supp. Fig. 8). The stronger impact of SOM photo-hyperpolarization on cortical responses to large stimuli is thus consistent with the preferential activation of SOMs by large stimuli (Fig. 1c). Thus, by inhibiting layer 2/3 neurons as a function of stimulus size SOMs generate an inhibitory surround (Fig. 4g).

Discussion

This study describes a cortical circuit that significantly contributes to surround suppression of layer 2/3 cells and identify a specific type of inhibitory neuron, the SOM, as a key mediator of this phenomenon. This circuit is thus likely to be involved in the contextual modulation of cortical responses to visual stimuli. The differential recruitment of PCs in superficial layers by ascending inputs and of SOMs by horizontal inputs underscores the fact that distinct neuron types are differentially integrated in the excitatory cortical circuit. These differences lead to different tuning properties as highlighted here by the distinct size-tuning curves. Thus, while small stimuli efficiently drive layer 2/3 PCs through the activation of ascending vertical inputs, SOMs, by summing activity in space via horizontal inputs, are preferentially driven by larger stimuli. As a consequence, the larger the stimulus, the stronger the SOM mediated suppression of PCs.

How can SOMs increase their firing as a function of stimulus size if they suppress layer 2/3 PCs, i.e. their main source of excitation? It is likely that the number of PCs recruited by the outer edge of the stimulus (an annulus that grows linearly with the diameter of the stimulus) more than compensate for the reduction in PC firing at the center of the stimulus.

Photo-hyperpolarization of SOMs reduces but does not abolish surround suppression. While this may be due in part to incomplete silencing of SOMs, surround suppression is also likely relayed to cortical layer 2/3 by earlier stages of visual processing [13–17] and other types of inhibitory neurons [21] or circuits [19] may also contribute to surround suppression.

The preferential recruitment of SOMs by horizontal excitatory projections is consistent with the long hypothesized role of these projections in size tuning [2]. In cortical layers with less extensive horizontal connectivity, size tuning may rely on different mechanisms [19, 20] or be entirely inherited from pre-cortical areas [15–17]. Importantly, because SOMs are tuned to the orientation of visual stimuli [35], they could account for the orientation dependence of surround suppression[8, 9, 36]. Furthermore, SOMs may respond differentially to specific stimulus properties, like contrast, and thus also contribute to the contrast dependence of surround suppression [9, 37, 38]. It is likely that a connectivity pattern similar to what is described here may be present in other cortical areas as well, and thus contribute to suppressive surround in several sensory and non-sensory modalities.

Methods Summary

Experiments were performed in accordance to the regulations of the IACUC at UCSD. Mice (except for Fig. 3a,b) were heterozygous for SOM-IRES-CRE (Jackson lab stock #013044) or PV-CRE (#008069) and the reporter allele Rosa-LSL-tdTOMATO (Allen Institute line Ai9, Jackson Labs #007905). For Fig. 3a,b mice were positive for Scnn1a-tg3-CRE (Jackson labs #009613) and crossed with to the Gin (#003718) or B13 line. For *in vivo* experiments mice were implanted with a custom head plate and habituated to head-fixation while running on a free spinning circular treadmill. For targeted recording *in vivo* tdTomato-expressing neurons were visualized by two photon microscopy and contacted by a glass electrode containing Alexfluor 488. Extracellular unit recording was performed via 16 channel silicon probes (Neuronexus). Single units were isolated using custom spike sorting software (Kleinfeld lab). We conditionally expressed ChR2 by *in utero* electroporation (for layer 2/3) or via a CRE-depednent AAV in Scnn1a-tg3-CRE (for layer 4). Arch or eNpHR were expressed via CRE-dependent AAVs in SOM- and PV-IRES-CRE mice. Visual stimuli were generated by custom software (Psych Toolbox) and presented on a gamma-corrected LCD monitor 15 cm from the mouse. Photostimulation *in vivo* was performed via fiber-coupled LEDs (Doric lenses). Photostimulation in vitro was via a combination of fiber-coupled LEDs, or LEDs mounted and coupled to an epifluorescence microscope (Olympus BX51).

eNpHR was activated by a shuttered arc-lamp. Slice preparation and intracellular recording followed previous protocols. Data acquisition, visual stimulation, and statistical analysis was performed in the Igor Pro and Matlab environments.

Supplementary Material

Refer to Web version on PubMed Central for supplementary material.

Acknowledgments

We thank J. Evora for the reconstruction of SOMs and technical assistance. We thank C. Niell and M. Stryker for providing expertise and sharing code used at the initial stages of this project. We thank Shawn Olsen for providing the firing rates of part of the units isolated under anesthesia. We thank P. Abelkop, and A. Linder for technical assistance. We thank J. Isaacson and members of the Scanziani lab for helpful advice. H.A.A. was supported by the Helen Hay Whitney Foundation and HHMI. W.B. and M.S. were supported by HHMI, the Gatsby charitable foundation and NIH grant NS069010.

References

1. Allman J, Miezin F, McGuinness E. Direction- and velocity-specific responses from beyond the classical receptive field in the middle temporal visual area (MT). Perception. 1985; 14:105–126. [PubMed: 4069941]
2. Angelucci A, Bressloff PC. Contribution of feedforward, lateral and feedback connections to the classical receptive field center and extra-classical receptive field surround of primate V1 neurons. Prog Brain Res. 2006; 154:93–120. [PubMed: 17010705]
3. Gilbert CD, Das A, Ito M, Kapadia M, Westheimer G. Spatial integration and cortical dynamics. Proc Natl Acad Sci U S A. 1996; 93:615–622. [PubMed: 8570604]
4. Hubel DH, Wiesel TN. Receptive Fields And Functional Architecture In Two Nonstriate Visual Areas (18 And 19) Of The Cat. J Neurophysiol. 1965; 28:229–289. [PubMed: 14283058]
5. Blakemore C, Tobin EA. Lateral inhibition between orientation detectors in the cat's visual cortex. Exp Brain Res. 1972; 15:439–440. [PubMed: 5079475]
6. Nelson JI, Frost BJ. Orientation-selective inhibition from beyond the classic visual receptive field. Brain Res. 1978; 139:359–365. [PubMed: 624064]
7. DeAngelis GC, Freeman RD, Ohzawa I. Length and width tuning of neurons in the cat's primary visual cortex. J Neurophysiol. 1994; 71:347–374. [PubMed: 8158236]
8. Knierim JJ, van Essen DC. Neuronal responses to static texture patterns in area V1 of the alert macaque monkey. J Neurophysiol. 1992; 67:961–980. [PubMed: 1588394]
9. Levitt JB, Lund JS. Contrast dependence of contextual effects in primate visual cortex. Nature. 1997; 387:73–76. [PubMed: 9139823]
10. Lamme VA. The neurophysiology of figure-ground segregation in primary visual cortex. J Neurosci. 1995; 15:1605–1615. [PubMed: 7869121]
11. Dobbins A, Zucker SW, Cynader MS. Endstopped neurons in the visual cortex as a substrate for calculating curvature. Nature. 1987; 329:438–441. [PubMed: 3657960]
12. Mareschal I, Shapley RM. Effects of contrast and size on orientation discrimination. Vision Res. 2004; 44:57–67. [PubMed: 14599571]
13. Solomon SG, Lee BB, Sun H. Suppressive surrounds and contrast gain in magnocellular-pathway retinal ganglion cells of macaque. J Neurosci. 2006; 26:8715–8726. [PubMed: 16928860]
14. Alitto HJ, Usrey WM. Origin and dynamics of extraclassical suppression in the lateral geniculate nucleus of the macaque monkey. Neuron. 2008; 57:135–146. [PubMed: 18184570]
15. Murphy PC, Sillito AM. Corticofugal feedback influences the generation of length tuning in the visual pathway. Nature. 1987; 329:727–729. [PubMed: 3670375]
16. Sceniak MP, Chatterjee S, Callaway EM. Visual spatial summation in macaque geniculocortical afferents. J Neurophysiol. 2006; 96:3474–3484. [PubMed: 16928793]

17. Bonin V, Mante V, Carandini M. The suppressive field of neurons in lateral geniculate nucleus. J Neurosci. 2005; 25:10844–10856. [PubMed: 16306397]
18. Ozeki H, et al. Relationship between excitation and inhibition underlying size tuning and contextual response modulation in the cat primary visual cortex. J Neurosci. 2004; 24:1428–1438. [PubMed: 14960615]
19. Bolz J, Gilbert CD. Generation of end-inhibition in the visual cortex via interlaminar connections. Nature. 1986; 320:362–365. [PubMed: 3960119]
20. Ozeki H, Finn IM, Schaffer ES, Miller KD, Ferster D. Inhibitory stabilization of the cortical network underlies visual surround suppression. Neuron. 2009; 62:578–592. [PubMed: 19477158]
21. Haider B, et al. Synaptic and network mechanisms of sparse and reliable visual cortical activity during nonclassical receptive field stimulation. Neuron. 65:107–121. [PubMed: 20152117]
22. Niell CM, Stryker MP. Highly selective receptive fields in mouse visual cortex. J Neurosci. 2008; 28:7520–7536. [PubMed: 18650330]
23. Van den Bergh G, Zhang B, Arckens L, Chino YM. Receptive-field properties of V1 and V2 neurons in mice and macaque monkeys. J Comp Neurol. 518:2051–2070. [PubMed: 20394058]
24. Margrie TW, et al. Targeted whole-cell recordings in the mammalian brain in vivo. Neuron. 2003; 39:911–918. [PubMed: 12971892]
25. Kawaguchi Y, Kubota Y. GABAergic cell subtypes and their synaptic connections in rat frontal cortex. Cereb Cortex. 1997; 7:476–486. [PubMed: 9276173]
26. McCormick DA, Connors BW, Lighthall JW, Prince DA. Comparative electrophysiology of pyramidal and sparsely spiny stellate neurons of the neocortex. J Neurophysiol. 1985; 54:782–806. [PubMed: 2999347]
27. Taniguchi H, et al. A resource of Cre driver lines for genetic targeting of GABAergic neurons in cerebral cortex. Neuron. 71:995–1013. [PubMed: 21943598]
28. Boyden ES, Zhang F, Bamberg E, Nagel G, Deisseroth K. Millisecond-timescale, genetically targeted optical control of neural activity. Nat Neurosci. 2005; 8:1263–1268. [PubMed: 16116447]
29. Petreanu L, Mao T, Sternson SM, Svoboda K. The subcellular organization of neocortical excitatory connections. Nature. 2009; 457:1142–1145. [PubMed: 19151697]
30. Adesnik H, Scanziani M. Lateral competition for cortical space by layer-specific horizontal circuits. Nature. 464:1155–1160. [PubMed: 20414303]
31. Wang Q, Burkhalter A. Area map of mouse visual cortex. J Comp Neurol. 2007; 502:339–357. [PubMed: 17366604]
32. Kapfer C, Glickfeld LL, Atallah BV, Scanziani M. Supralinear increase of recurrent inhibition during sparse activity in the somatosensory cortex. Nat Neurosci. 2007; 10:743–753. [PubMed: 17515899]
33. Chow BY, et al. High-performance genetically targetable optical neural silencing by light-driven proton pumps. Nature. 463:98–102. [PubMed: 20054397]
34. Atasoy D, Aponte Y, Su HH, Sternson SM. A FLEX switch targets Channelrhodopsin-2 to multiple cell types for imaging and long-range circuit mapping. J Neurosci. 2008; 28:7025–7030. [PubMed: 18614669]
35. Ma WP, et al. Visual representations by cortical somatostatin inhibitory neurons--selective but with weak and delayed responses. J Neurosci. 30:14371–14379. [PubMed: 20980594]
36. Cavanaugh JR, Bair W, Movshon JA. Selectivity and spatial distribution of signals from the receptive field surround in macaque V1 neurons. J Neurophysiol. 2002; 88:2547–2556. [PubMed: 12424293]
37. Kapadia MK, Westheimer G, Gilbert CD. Dynamics of spatial summation in primary visual cortex of alert monkeys. Proc Natl Acad Sci U S A. 1999; 96:12073–12078. [PubMed: 10518578]
38. Sceniak MP, Ringach DL, Hawken MJ, Shapley R. Contrast's effect on spatial summation by macaque V1 neurons. Nat Neurosci. 1999; 2:733–739. [PubMed: 10412063]

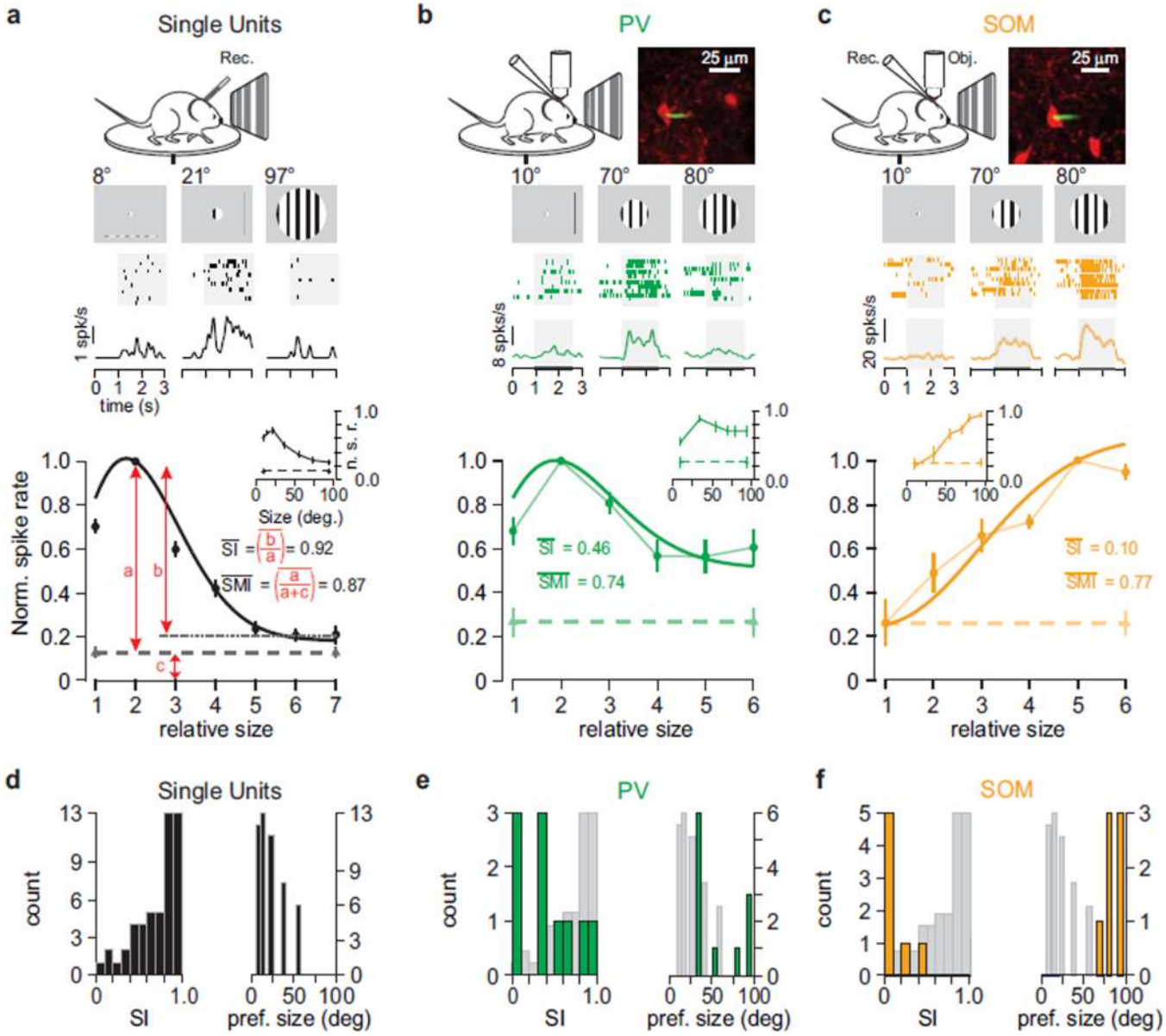

Fig. 1. Different size tuning of three types of neurons in the visual cortex

a) Top: Schematic of the experimental setup. Center: Response of example unit to visual stimuli of three different sizes (top row: Raster plot; bottom row: PSTH). Shaded area represents period of stimulus presentation. Bottom: Average size tuning curve of 53 peak-aligned and normalized single units (6 animals, 11 recording sessions). Gray triangles and a dashed line: baseline firing rate. Inset: Average of the normalized but not peak-aligned 53 size tuning curves.

b) Top left: Schematic of the experimental setup. Top right: td-Tomato expressing PV (red) with attached Alexafluor 488 filled recording pipette (green). Center: Response of PV to visual stimuli of three different sizes (top row: Raster plot; bottom row: PSTH). Bottom: Average size tuning curve (n = 11 peak-aligned and normalized size tuning curves; 3 animals). Inset: Average of the normalized but not peak-aligned 11 size tuning curves.

c) As in (b) but for SOMs (n=7; 4 animals).

d)– f) Distribution of SIs (left panels) and of preferred stimulus sizes (right panels) for single units (d), PVs (e) and SOMs (f). The SOM and PV data are superimposed onto the single unit data (gray, from (e)) for comparisons. All error bars are s.e.m.

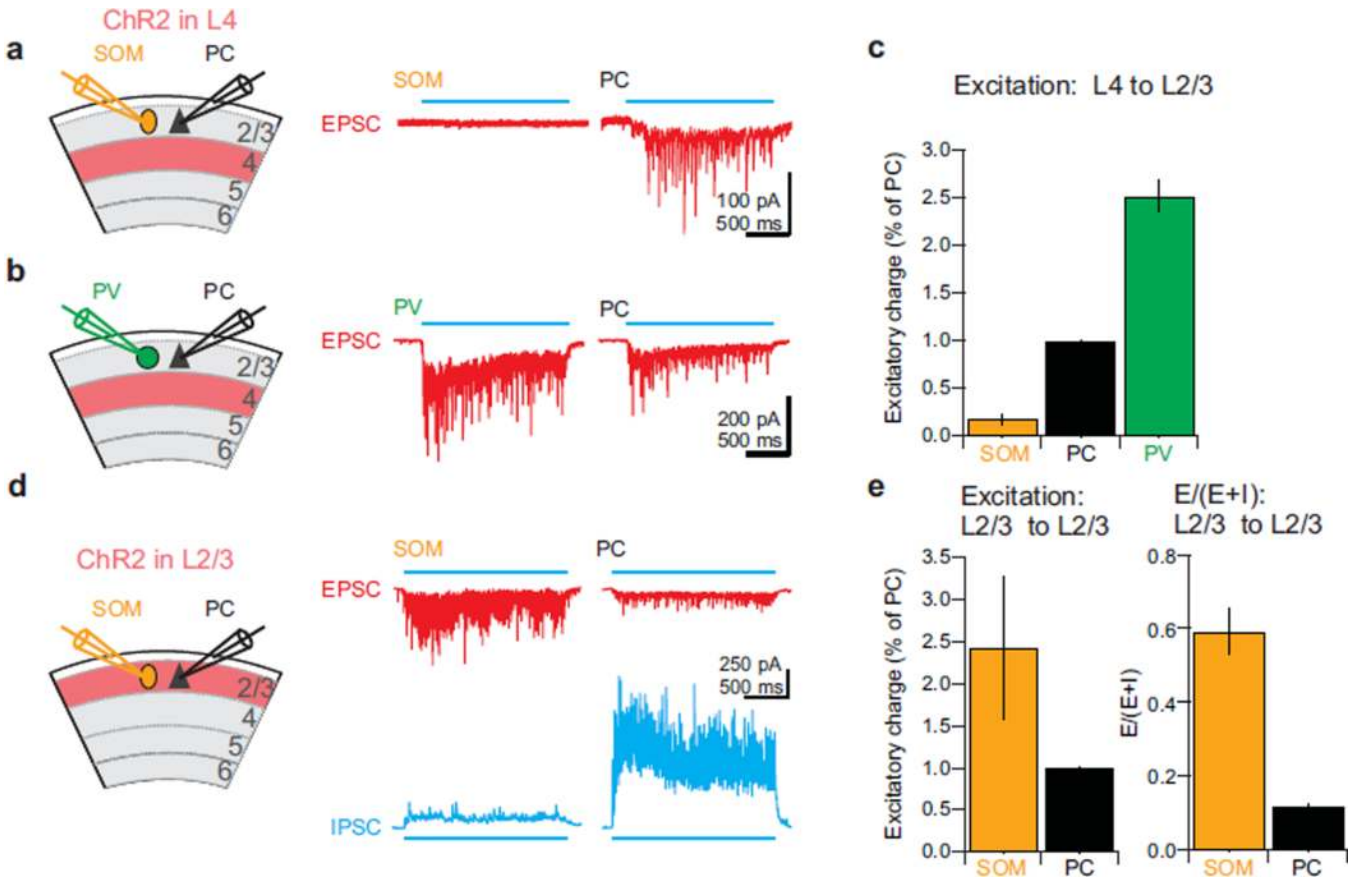

Fig. 2. SOMs are selectively excited by horizontal cortical projections

a)Left: Schematic of the experimental setup. ChR2 is expressed selectively in layer 4 excitatory neurons. Recording electrodes in layer 2/3 target a SOM (orange) and a pyramidal cell (PC, black). Right: Excitatory currents simultaneously recorded in a SOM and a PC in response to photo-stimulation of layer 4 with a ramp of blue light (horizontal blue line).

b)Left: Schematic of the experimental setup. As in (a) but whole cell recording electrodes in layer 2/3 target a PV (green) and a PC (black). Right: Excitatory currents simultaneously recorded in a PV and a PC in response to photo-stimulation of layer 4 as in (a).

c)Summary statistics of the excitatory charge (as a fraction of that simultaneously recorded in the PC) recorded in SOMs (n=8) and PVs (n=8); $p<0.05$.

d)Left: Schematic of the experimental setup. As in (a) except ChR2 is expressed selectively in PCs of layer 2/3. Right, excitatory (red, top traces) and inhibitory (bottom, blue traces) currents simultaneously recorded in a SOM and a PC in response to photo-stimulation of layer 2/3 with a ramp of blue light.

e)Left: Summary statistics of excitatory charge (as a fraction of that simultaneously recorded in the PC) recorded in SOMs as compared to layer 2/3 PCs (n=7, $p<0.05$). Right: Ratio of excitation to inhibition (expressed as E/E+I) recorded in SOMs and PCs (n=10, $p<0.05$). All error bars are s.e.m.

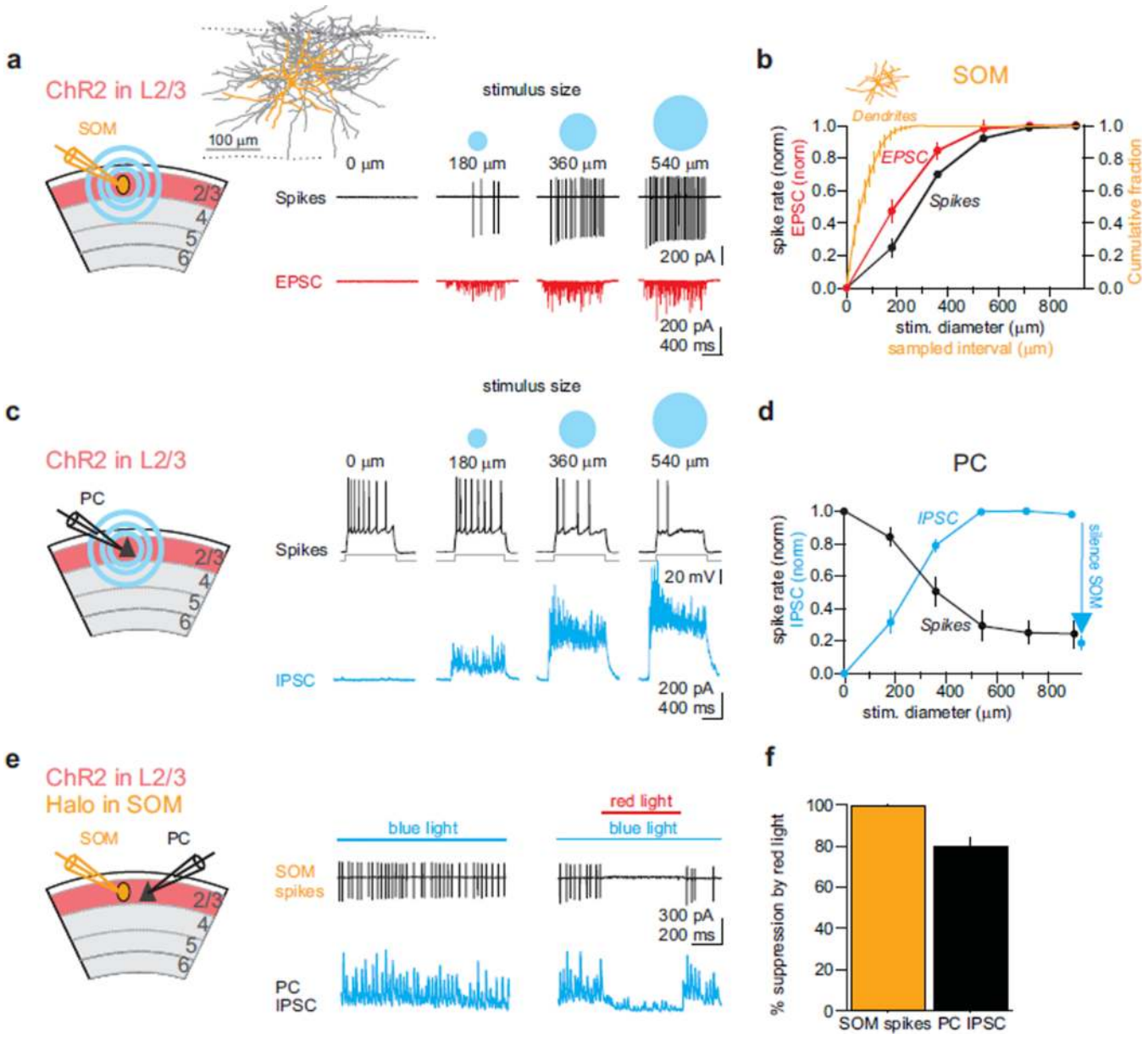

Fig. 3. Suppression of PCs by SOMs as a function of the activated layer 2/3 area

a) Left: Schematic of the experimental setup Inset: Anatomical reconstruction of a biocytin-filled layer 2/3 SOM; dendrites: orange; axon: gray; dotted lines: top: border with layer 1; bottom: border with later 4. Right: Action potentials (black traces, top) recorded in the cell-attached mode in a SOM in response to light spot sizes of increasing diameter. Bottom: Excitatory currents (red traces) recorded subsequently in the whole cell voltage clamp configuration in the same SOM neuron in response to the same photo-stimuli.

b) Summary graph for the spiking (black; n =14) and excitatory charge (red; n=6) of SOMs in response to light spots of five different diameters. Orange: summary statistics of the cumulative fraction of SOM dendritic arbor length within a sampled horizontal interval centered on the SOM cell body (n = 6). Inset: dendrites of the SOM illustrated in (a) but scaled to x-axis.

c) Left: Schematic of the experimental setup. As in (a) but recording from PC. Right, top: Spiking of PC recorded in current clamp mode (black traces) in response to depolarizing

current steps while layer 2/3 is photo-stimulated with increasingly large blue light spots. Bottom: Inhibitory currents recorded in a PC to the same light stimuli.
d) Summary graph of the suppression of firing of PCs (black, n=7) and intracellularly recorded inhibitory charge (blue, n=6) to light spots of five different diameters. Photo-hyperpolarizing SOMs (blue arrow; see (e) below) reduces inhibitory charge in PCs.
e) Schematic of the experimental setup. ChR2 is expressed in a fraction of layer 2/3 PCs and halorhodopsin is conditionally expressed in SOMs. Recording electrodes target a SOM (orange) and a PC (black). Full field blue light activates layer 2/3 PCs, while red light suppress SOMs. Traces: Spikes (black traces, top) recorded in the cell-attached mode in a SOM and inhibitory currents (blue traces, bottom) simultaneously recorded in a voltage clamped PC in response to blue light photo-stimulation (blue bar) of layer 2/3. Simultaneous illumination with red light (red bar, right panel) to photo-hyperpolarize SOMs abolishes SOM firing (left) and reduces inhibitory currents in the PC (right; see also blue arrow in (d)).
f) Summary graph for halorhodopsin-mediated reduction of SOM firing (n=6) and concomitant reduction in inhibitory charge (IPSC) in layer 2/3 PCs (n=8).

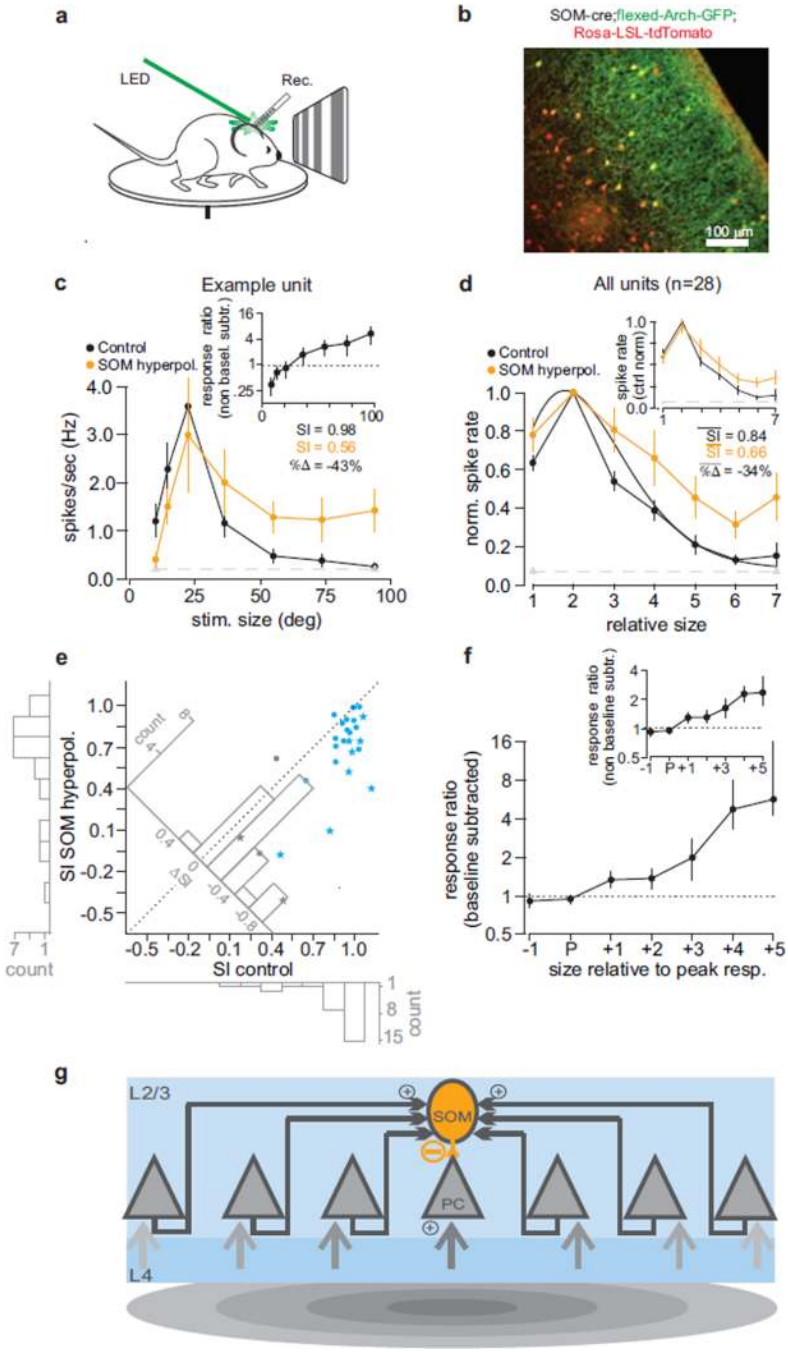

Fig. 4. SOMs contribute to size tuning of layer 2/3 PCs

a) Schematic of the experimental setup.

b) Section of the visual cortex of a SOM-CRE;Rosa-LSL-tdTomato mouse injected with AAV-flexed-Arch-GFP. All SOM-CRE cells express tdTomato (red) and infected neurons also express Arch-GFP (green).

c) Size tuning of an isolated unit in control (black) and during photo-hyperpolarization of SOMs (orange). Dashed line is baseline firing rate; Inset: response ratio for this example unit. All error bars are s.e.m.

d) Average peak-aligned and scaled size tuning curves for 28 isolated single units (3 animals; 7 recording sessions). Black: Control conditions; orange: SOM hyperpolarization.

Inset: Average peak-aligned and control normalized size tuning curve where the SOM-hyperpolarization condition (orange curve). Note the lack of facilitation at the preferred or smaller size. All error bars are s.e.m.

e) Scatter plot: SI under control conditions (x-axis) plotted against SI under SOM hyperpolarization (y-axis) for each of the 28 units. Blue data points are units that are size tuned at baseline (n=24, SI > 0; $p<0.05$). Gray data points are units not sized tuned at baseline. Stars are units that showeda significant reduction in SI (n=10; $p<0.05$). Histograms beside×and y-axes show SI distribution under control and SOM hyperpolarization, respectively. Oblique histogram illustrates the distribution of changes in SI with SOM hyperpolarization.

f) The ratio of the average response during SOM photo-hyperpolarization to the average response under control conditions plotted against stimulus size relative to peak. Same units as (d) Inset: the same ratio without subtracting the baseline firing rate.

g) Schematic illustration of the cortical circuit in layer 2/3 contributing to surround suppression. As a visual stimulus expands (shades of gray), recruitment of adjacent PCs increases SOM excitation through horizontal axons (horizontal arrows).